



Nonlinear seismic analysis of perforated steel plate shear walls



Anjan K. Bhowmick^{a,*}, Gilbert Y. Grondin^b, Robert G. Driver^c

^a Department of Building, Civil and Environmental Engineering, Concordia University, Montreal, QC, Canada

^b AECOM, Edmonton, AB, Canada

^c Department of Civil and Environmental Engineering, University of Alberta, Edmonton, AB, Canada

ARTICLE INFO

Article history:

Received 5 December 2012

Accepted 13 November 2013

Available online 15 December 2013

Keywords:

Steel plate shear wall

Seismic analysis

Circular perforations

ABSTRACT

The behaviour of unstiffened steel plate shear walls with circular perforations in the infill plates is examined. A shear strength model of the infill plate with multiple circular openings is proposed based on a strip model. Eight perforation patterns in a single storey steel plate shear wall of two different aspect ratios were analyzed using a geometric and material non-linear finite element model to assess the proposed shear strength model. A comparison between the nonlinear pushover analysis and the proposed shear strength equation shows excellent agreement. The proposed model is used to design the boundary columns of three sample four-storey perforated shear walls. A comparison between the predicted design forces in the boundary columns for the selected shear walls with the forces obtained from nonlinear seismic analyses demonstrates the accuracy of the proposed simple model to predict the design forces in the columns.

© 2013 Elsevier Ltd. All rights reserved.

1. Introduction

Unstiffened steel plate shear walls have been in use for a long time. Properly designed steel plate shear walls (SPSW) have high ductility, high initial stiffness, high redundancy, and excellent energy absorption capacity. Most recent practice for SPSW is to use thin unstiffened plates for the infill panels, relying on tension field action to provide lateral load resistance. For seismic design, the surrounding framing members are generally “capacity designed”, i.e., they are designed to develop the full capacity of the infill plate tension field, while they remain essentially elastic.

The thickness of the infill plate used in a SPSW is often governed by factors other than strength (e.g. handling and welding), which often results in much stronger shear walls than required for lateral load resistance. This creates a problem in capacity design, as it introduces excessive design forces to the surrounding frame members, thus increasing their required size. Recent attempts to address this problem have included the use of light-gauge, cold-formed, steel infill plates or low yield strength (LYS) steel for infill plates [1,2], introducing vertical slits in the infill plate [3,4], or introducing a regular pattern of circular perforations in the infill plate [2]. Among all these methods of weakening the infill plate, the perforated SPSW proposed by Vian [2], illustrated in Fig. 1, represents an attractive system since it also provides a route for the utility systems to pass through the infill plates.

Research on circular perforations in shear panels started with Roberts and Sabouri-Ghomi [5]. They conducted a series of quasi-static tests under cyclic diagonal loading on unstiffened steel plate shear

panels with centred circular openings. The following approximate equation was proposed for the calculation of the strength of an unstiffened infill panel with a central circular opening:

$$V_{op} = V_p \left(1 - \frac{D}{d_p} \right) \quad (1)$$

where V_{op} and V_p are the strength of a perforated and a solid shear panel, respectively, D is the perforation diameter, and d_p is the panel height.

Purba [6] analyzed a 4000 mm by 2000 mm single storey SPSW with multiple regularly-spaced circular perforations of equal diameter. An investigation of the effect of infill plate thickness and perforation diameter on the shear strength indicated that Eq. (1) provides a conservative estimate of the strength of perforated infill plates with multiple perforations when d_p in Eq. (1) is replaced by S_{diag} , the diagonal distance between each perforation line (see Fig. 1). Through a calibration study, the following modified equation was proposed to calculate the shear strength of perforated SPSWs with the regular perforation pattern used by Vian [2]:

$$V_{op} = V_p \left(1 - 0.7 \frac{D}{S_{diag}} \right). \quad (2)$$

Purba [6] also found that results from an individual perforated strip analysis can accurately predict the behavior of a complete SPSW with perforations provided that the hole diameter is less than 60% of the strip width, namely, $\left(\frac{D}{S_{diag}} \leq 0.6 \right)$. Although Eq. (2) was found to provide good strength predictions of SPSWs for the regular perforation

* Corresponding author. Tel.: +1 514 848 2424; fax: +1 514 848 7965.

E-mail address: anjan.bhowmick@concordia.ca (A.K. Bhowmick).

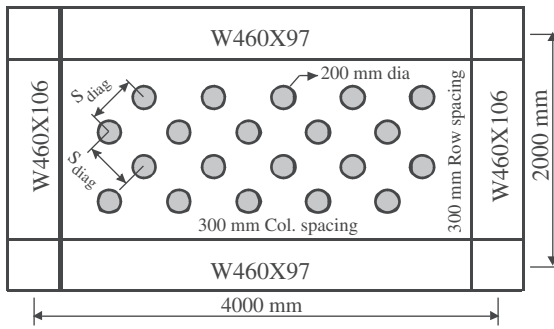


Fig. 1. Test specimen from Vian [2].

pattern proposed by Vian [2], a more general expression, applicable to any pattern of perforations, is clearly desirable.

This paper presents a general equation for determining the strength of perforated SPSWs. The proposed equation is based on a strip model, and is derived by discounting the strips that are intercepted by perforations. Finite element models of two single storey SPSWs (with aspect ratios of 2.0 and 1.5) and with eight different types of perforation patterns are analyzed to investigate the effectiveness of the proposed equation.

AISC Steel Design Guide 20 [7] presents a capacity design method for the design of SPSW with solid infill plates. The method assumes that all the infill plates over the building height reach their full yield capacity and plastic hinges develop at the ends of all the horizontal members of the frame. The columns axial forces are a function of the tension field in the infill plates and the bending moments and shear forces in the beams. The presence of perforations in the infill plates affects the forces and moments in the boundary columns, thus requiring modifications to the current design method. This paper proposes modifications to the capacity design method to accommodate SPSWs with circular perforations. The use of the modified capacity design method is illustrated on three SPSWs with circular perforations. The design force effects in the boundary columns are compared with the design forces obtained from a seismic analysis of the 4-storey SPSWs under four spectrum-compatible earthquake ground motions for Vancouver, Canada.

2. Strength prediction of perforated infill plate

To develop a general strength model, it is assumed that the infill plate has negligible buckling capacity and that the shear strength of the SPSW is provided strictly by tension field action. The angle of the tension field, α , is obtained from the equation specified both in Canadian standard CAN/CSA-S16-09 [8] and in the AISC seismic Specification [9]. In the presence of a circular hole of diameter D , as shown in Fig. 2, one can discount part of the contribution, β , of the steel within a

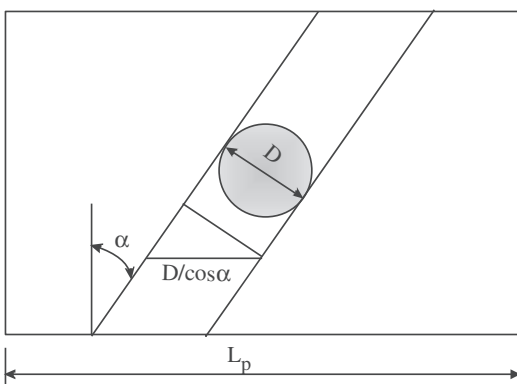


Fig. 2. Strip model for perforated infill plate.

diagonal strip of width D [2]. Taking the diagonal strip containing the circular hole to be at the angle of the tension field, α , the horizontal projection of the portion of the strip to be discounted is $\beta \frac{D}{\cos \alpha}$. The effective width of a perforated infill plate, $L_{p,eff}$, accounting for the presence of a single circular perforation or multiple perforations affecting only one strip, is:

$$L_{p,eff} = L_p - \beta \frac{D}{\cos \alpha} \quad (3)$$

where L_p is the width of infill plate.

When more than one strip is affected by perforations, the effective width of the perforated infill plate, $L_{p,eff}$, is

$$L_{p,eff} = \left(L_p - N_r \beta \frac{D}{\cos \alpha} \right) \quad (4)$$

where N_r is the maximum number of diagonal strips (counted at any section cut parallel to length L_p) with circular perforations to be discounted.

It is assumed that all the strips with perforations are inclined by the same angle. Also, Eq. (4) assumes that all the perforations have same diameter. In case of different perforation diameters, Eq. (4) can be modified as:

$$L_{p,eff} = \left(L_p - \sum_{i=1}^{N_r} \beta \frac{D_i}{\cos \alpha} \right) \quad (5)$$

For this study, perforations with same diameters will be considered and thus Eq. (4) will be used for the development of shear strength equation for perforated infill plate.

The shear strength of a solid infill plate, V_p , is given by [10]:

$$V_p = 0.5 \sigma w L_p \sin 2\alpha \quad (6)$$

Thus, the shear strength of a perforated infill plate, V_{op} is

$$V_{op} = 0.5 \sigma w L_{p,eff} \sin 2\alpha \quad (7)$$

where w is the infill plate thickness and σ is the stress in the infill plate tension strips, taken as the material yield strength for design.

From Eqs. (6) and (7)

$$\frac{V_{op}}{V_p} = \left(1 - \beta N_r \frac{D}{L_p \cos \alpha} \right) \quad (8)$$

The designer can estimate graphically the value of $N_r \frac{D}{L_p \cos \alpha}$ from the geometry of the SPSW. As discussed in the next section, the value of the perforated strip contribution, β , is derived from the analysis of a series of single storey SPSWs with a variety of circular perforation patterns.

3. Analysis of perforated steel plate shear walls

Nonlinear finite element analyses of a series of single-storey SPSWs were carried out using ABAQUS [11] to determine the magnitude of the constant β . Both material and geometric nonlinearities were considered. In total, eight different types of perforation patterns were considered in this study. Variation in perforation diameters was also considered for each type of perforation pattern.

3.1. Selection of shear wall system

The single-storey SPSW considered here is part of a hypothetical symmetrical office building located in Vancouver, Canada. The 3.8 m tall building has a floor area of 2014 m². As shown in Fig. 3, the building

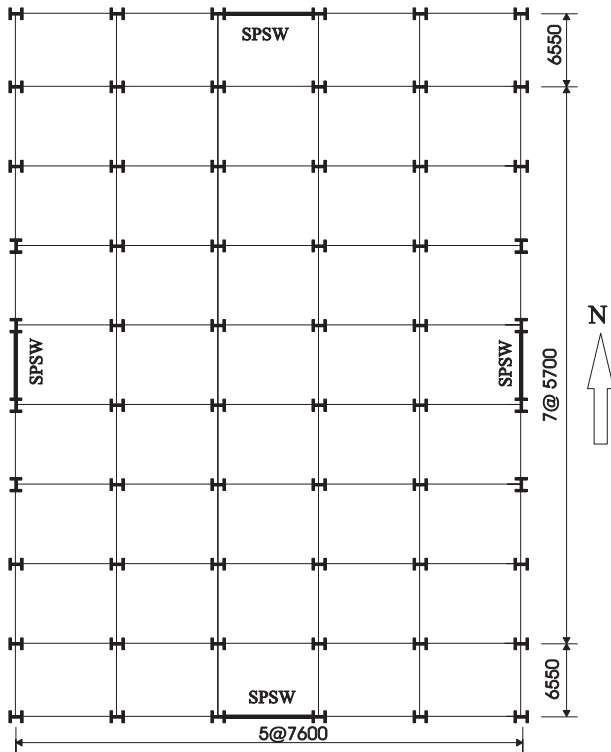


Fig. 3. Plan view of sample building.

has two SPSWs in each direction to resist lateral loads. For simplicity, torsional effects on the building are ignored and each shear wall is assumed to resist half of the design seismic forces. The shear walls in the East–West direction are 7.6 m wide, resulting in a panel aspect ratio of 2.0. The building is assumed to be founded on rock (site class B according to NBCC 2010). The roof dead load and snow load are 1.12 kPa and 1.48 kPa, respectively. NBCC 2010 [12] load combination $D + 0.5L + E$ (where D = dead loads, L = live loads and E = earthquake loads) is used for intermediate floors and for the roof, the load combination $D + 0.25S + E$ (where S = snow loads) was considered. The design seismic base shear is obtained using the equivalent static force procedure of the National Building Code of Canada (NBCC) 2010 [12]. An importance factor, I , of 1.0 is assumed for the design. As prescribed by NBCC 2010, a ductility-related force modification factor, R_d , of 5.0 and an overstrength force modification factor, R_o , of 1.6 are used in the design.

An infill plate thickness of 3.0 mm is used. The value of the angle of the diagonal tension field is taken as 45° in this paper. The design of a SPSW is not sensitive to the angle of inclination of the tension field and values between 38° and 50° have been recommended [13]. With the angle of the tension field known, boundary beams, $W610 \times 498$, were selected to carry the forces from yielding of an infill plate without perforations. A $W360 \times 900$ section was selected for the columns to carry the forces developed in the yielded infill plate and the plastic hinges at the ends of the top beam.

Fig. 4 illustrates the eight perforation patterns used in this investigation. The perforations are placed in such a way so that the behaviour of the SPSWs remains symmetrical under the lateral loads applied from both directions. The figures also show the 45° strips drawn around the perforations. All the circular perforations shown in Fig. 4 have a diameter of 500 mm.

3.2. Characteristics of the finite element model

The infill plate, the beams and columns were modelled using a general purpose four-node, doubly-curved, shell element with reduced

integration (ABAQUS element S4R). The beams and columns were rigidly connected together and the infill plate was connected directly to the beams and columns. The columns were pinned at their base. Initial imperfections were applied in the model to help initiate buckling of the infill plate and subsequent development of the tension field. The initial imperfection pattern in the infill plate was taken as the first buckling mode of the plate wall with a peak amplitude of 1.0 mm. The finite element model used for this investigation was validated previously for SPSWs with solid infill plates for quasi-static cyclic analysis tests and dynamic test results [14]. Further validation of the model with circular perforations was conducted using the regularly spaced perforated SPSW test by Vian [2]. For this test, beams and columns had a specified yield strength of $F_y = 345$ MPa. The infill plate used had a thickness of 2.6 mm and had yield strength and tensile strength of 165 MPa and 305 MPa, respectively. As in the test, a controlled displacement was applied through the centre line of the top beam. The displacement was increased to a maximum value as obtained from the envelope of hysteresis curve of the physical test. The FE mesh of the perforated steel plate shear wall is shown in Fig. 5(a). The measured (as obtained from physical experimentation) and predicted (from FEA) base shear values are plotted against the overall storey displacement in Fig. 5(b). The figure indicates that the finite element model predicts the initial stiffness and post-yield response of the shear wall accurately. For the remaining finite element analyses, an elasto-plastic stress versus strain curve was adopted, with a modulus of elasticity of 200 000 MPa and a yield strength of 385 MPa for the infill plates, and 350 MPa for the beams and columns. A displacement control solution strategy where the top storey displacement was used as the control parameter was used in this work. A target maximum displacement of 110 mm was selected for all the pushover analyses of the single storey SPSWs.

3.3. Pushover analysis and results

SPSWs with the eight perforation patterns shown in Fig. 4, were modelled and analyzed. Fig. 6 shows the deformed mesh for the Type 5 perforation case. The light grey patches in this plot represent complete yielding whereas the dark grey areas represent material that has not yielded. Fig. 6 shows that a significant portion of the diagonal strips along the perforations is not effective (no yielding) and thus can be discounted.

A reference SPSW with a solid infill plate was also analyzed to compare the behaviour with perforated SPSWs. In order to compare only the infill plate strengths a model consisting of only the rigid frame was also analyzed. Shear strengths of 9771 kN and 6269 kN were obtained for the single storey SPSW with the solid infill plate and without any infill plate, respectively. Pushover curves for all eight perforation patterns displayed in Fig. 4 (with a perforation diameter of 500 mm) are presented in Fig. 7. To examine the effect of perforation diameter, all eight perforation patterns were re-analyzed for two other perforation diameters, namely, 400 mm and 600 mm. Resulting pushover curves are shown in Figs. 8 and 9. The curves for the solid plate and the bare frame cases provide the upper and lower bounds, respectively, for the perforation patterns considered.

Table 1 presents the shear capacity for all the perforation patterns. As expected, there is a reduction in the shear strength of the SPSW as the perforation diameter increases. Types 2, 3 and 4 SPSWs have only two circular perforations in different locations, which results in two discounted strips for each model. For any perforation diameter, the pushover analysis results show that the location of the perforations (in Type 2, 3, and 4) has only a small effect on the shear strength (less than 2% difference). For 400 mm and 500 mm holes, the variation in shear strength is less than 1%, and for the 600 mm diameter holes it is 1.3%. Since the Type 1 case has only one perforation at the centre of the infill plate, one strip can be discounted. It can be observed from Fig. 4 that for Type 5 and Type 8 perforation patterns some two strips that are slightly wider than the others and each

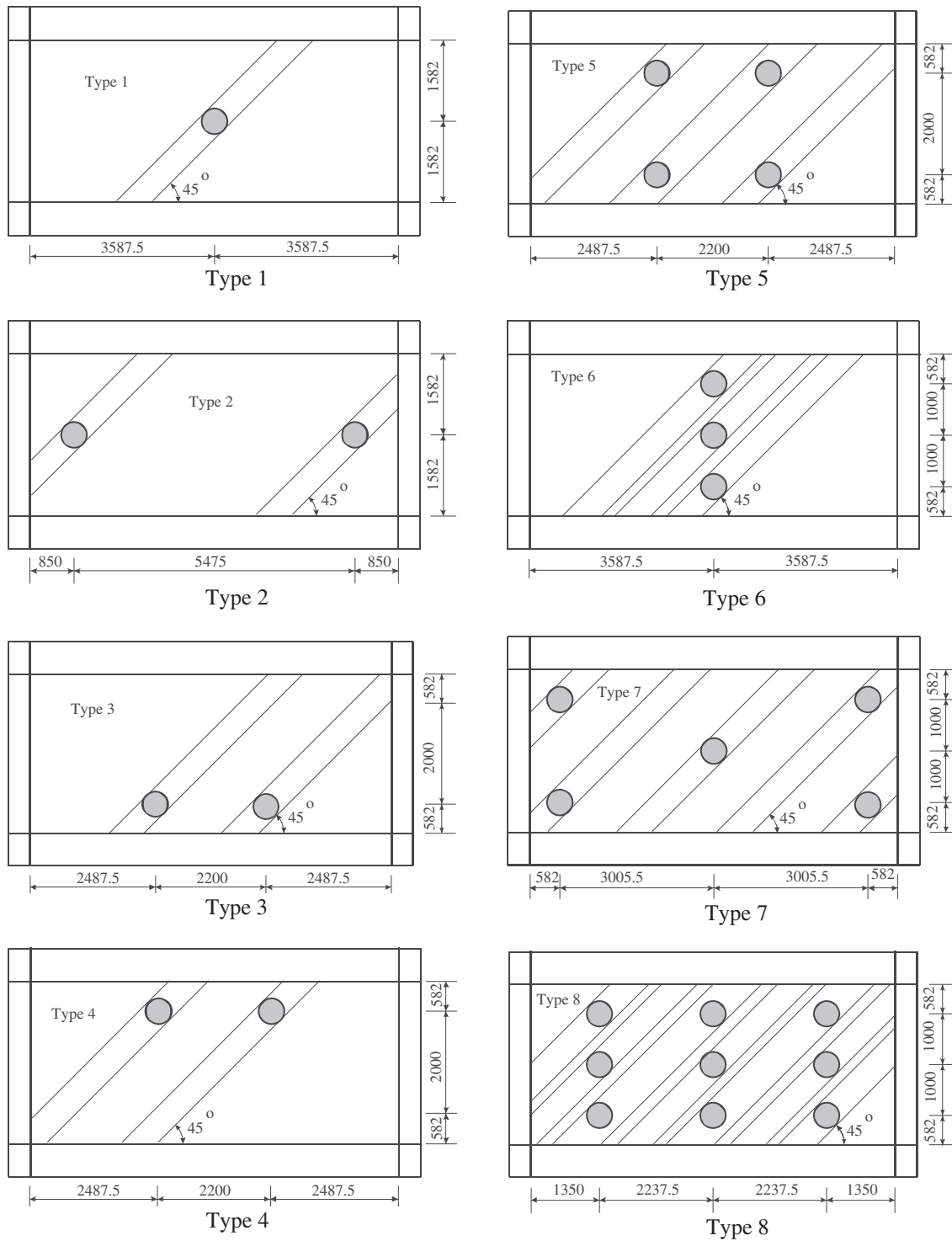
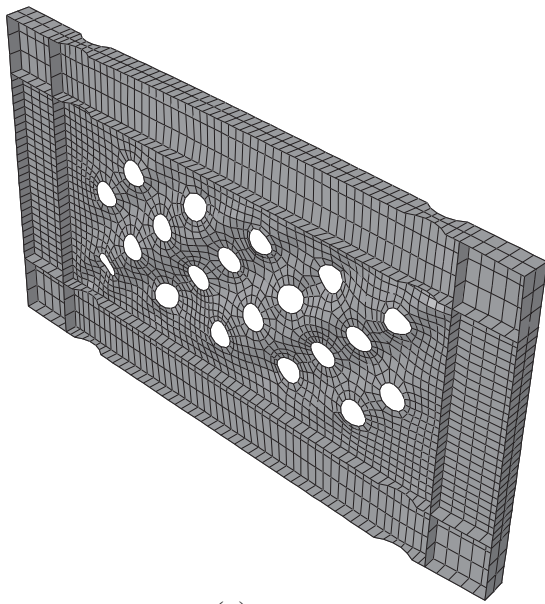


Fig. 4. Selected perforation layouts.

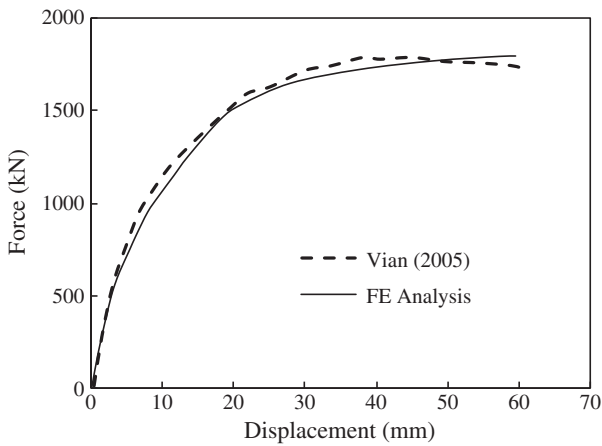
contain two perforations. For Type 5 and Type 8 perforation patterns, 3.3 and 7.3 equivalent strips are discounted. Since for Type 8 perforation pattern, maximum numbers of strips are discounted, for all three perforation diameters, the Type 8 perforation pattern results in a lower base shear strength than that of any other perforation types considered here.

By assuming that the SPSW shear strength can be taken as the summation of the frame shear strength and the infill plate shear strength, it is possible to obtain the infill plate strength by subtracting the bare frame strength from the total strength at the same displacement level,

namely, 110 mm, as selected here. This approximation which does not satisfy the compatibility of deformations at the frame and plate interface for the SPSW and bare frame system has previously been adopted in many research [2,6] and does not have any significant effect in the global behaviour of SPSW system. Ratios of perforated infill plate strengths to the solid infill plate strength, V_{op}/V_p , were calculated for all perforation configurations and are presented in Table 2. The number of diagonal strips to be discounted, N_r , is also presented in Table 2. The ratios of V_{op}/V_p for the three perforation diameters were then used in Eq. (8) to evaluate the constant β . The β values determined for the 24 cases



(a) FE mesh



(b) Pushover curve

Fig. 5. Validation of push over curve for Vian 4 specimen: (a) FEA mesh, (b) Pushover curve.

considered are plotted against V_{op}/V_p in Fig. 10. Except for the shear wall with a single perforation, Type 1 (where the values of β range from 1.3 to 1.4), the β values all lie between 0.6 and 0.8. For infill plates with a single hole, it was observed that more than the one strip containing the hole was ineffective, which is contrary to all the other cases.

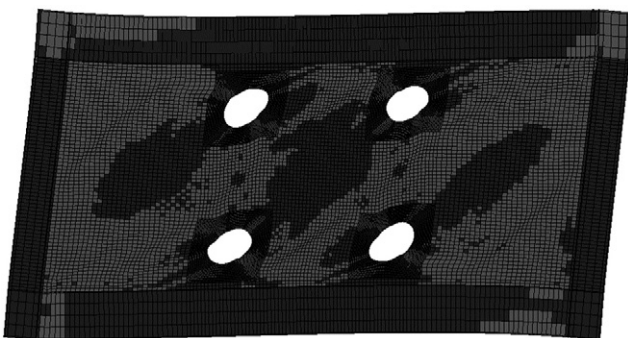


Fig. 6. Deformed FE mesh for Type 5 perforation.

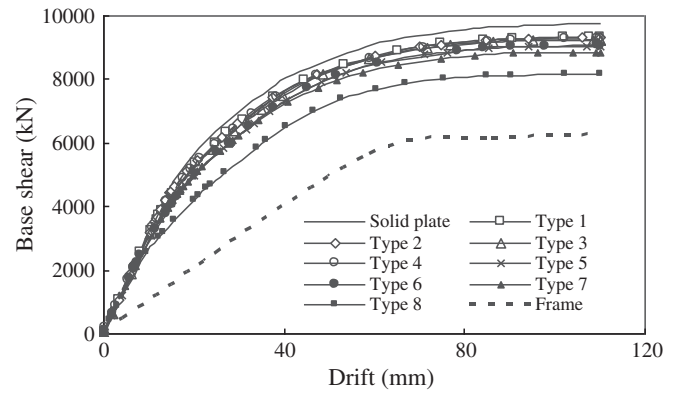


Fig. 7. Pushover curves for SPSW with 500 mm diameter perforations.

To investigate further the effect of a single perforation in the infill plate, plate walls similar to Type 2 and Type 3 were re-analyzed, but only with the left perforation. The ratio V_{op}/V_p for these two cases was 0.93 for both cases, which results in a value of β equal to 0.88. Thus, for the 400 mm diameter perforation, the shear strength of the infill plate reduced more (4.3% for the cases studied) when the single perforation is placed at the centre of the infill plate ($V_{op}/V_p = 0.89$, as shown in Table 2). Nevertheless, since there is only one hole, unless it is very large, the effect on the overall wall capacity is relatively small. The mean of all β values in Fig. 10, excluding the three values obtained for the infill plate with a single perforation at the centre, is 0.69. A value of 0.7 was selected for the constant β to calculate the ratio of perforated infill plate strength to the solid infill plate strength, V_{op}/V_p .

Fig. 11 presents ratios of perforated infill plate strengths to the solid infill plate strength, as determined from finite element analysis (FEA), compared to the ratios predicted using Eq. (8) as a function of the number of discounted strips, N_r . For all the cases, except the Type 1 cases, excellent agreement is observed between the FEA results and Eq. (8). For the Type 1 perforation pattern, when the value of 0.7 is used for β , Eq. (8) overestimates the value of V_{op}/V_p by only 6.4% for the 400 mm diameter case, 7.2% for the 500 mm diameter case, and 8.4% for the 600 mm diameter case.

Eq. (8), with the value of $\beta = 0.7$ as derived above, was used to predict the reduction in shear strength for a SPSW with an aspect ratio of 1.5. The single storey SPSW was designed for the same loading conditions as the SPSWs with an aspect ratio of 2.0. Again, an infill plate thickness of 3.0 mm was used. In this case, a beam section of W530x272 and a column section of W360x509 were selected. Similar eight perforation patterns, as analyzed for the SPSW with an aspect ratio 2.0, were also considered. The detailed layout for the perforation patterns for the SPSWs with an aspect ratio of 1.5 is presented elsewhere [15]. Nonlinear

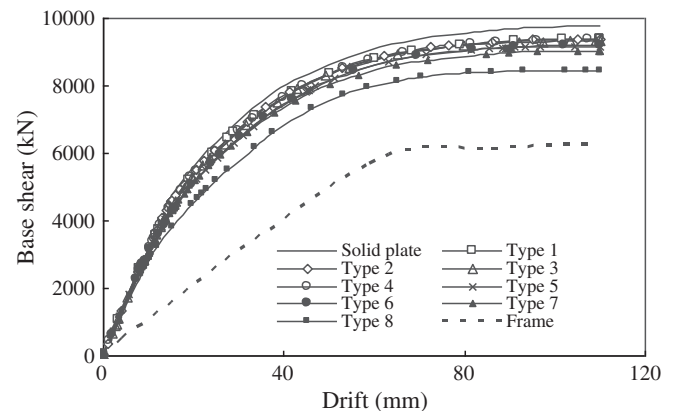


Fig. 8. Pushover curves for SPSW with 400 mm diameter perforations.

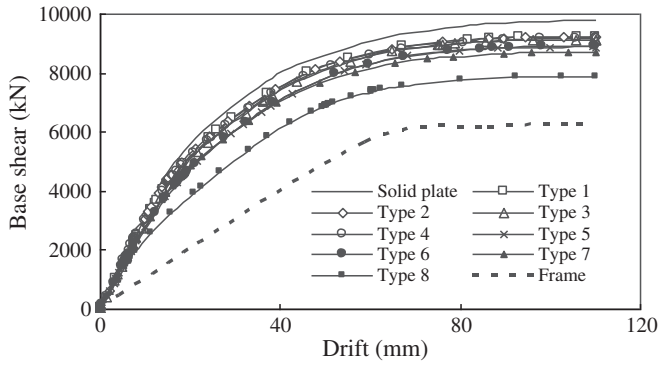


Fig. 9. Pushover curves for SPSW with 600 mm diameter perforations.

pushover analyses of all the eight perforation patterns were carried out for a storey drift of 110 mm. Ratios of perforated infill plate strengths to the solid infill plate strength, V_{op}/V_p , were calculated and are compared with the values obtained from Eq. (8) in Fig. 12. Again, excellent agreement between the finite element analysis results and those from Eq. (8) is observed.

Finally, Eq. (8) was used for the perforation pattern used by Vian [2] (shown in Fig. 1). A value of 6 was used for N_r in the proposed equation to reflect the presence of six diagonal rows of holes.

The equation proposed by Purba [6], Eq. (2), to determine the reduction in shear strength for this specific perforation layout, was compared with Eq. (8). Fig. 13 shows that for the regular perforation layout, the reduction in shear strength from predicted by Eq. (8), is nearly identical to that obtained from the equation recommended by Purba [6]. Thus, Eq. (8) can be used to predict the shear strength reduction of a SPSW with circular perforations.

4. Design of boundary columns of perforated steel plate shear walls

The capacity design method for design of columns of SPSWs with solid infill plates presented in AISC Steel Design Guide 20 [7] is modified here to include the effect of circular perforations. The modified design method is summarised as follows:

- (1) For a selected perforation layout, the ratio of perforated infill plate strength to the solid infill plate strength, V_{op}/V_p , is calculated using Eq. (8). It is suggested that the value of N_r be rounded to the lower integer. This is a conservative approach when the boundary columns are to be designed to yield the perforated infill plates.
- (2) The distributed loads developed from yielding of the perforated infill plates, as shown in the free body diagram in Fig. 14 of a typical column from an n-storey SPSW, can be obtained by multiplying the distributed loads developed from yielding of solid infill plates by V_{op}/V_p . Thus, the distributed loads applied

Table 1
Base shear capacity for different perforation patterns.

Perforation pattern	Shear strength (kN)		
	Perforation diameter		
	400 mm	500 mm	600 mm
Type 1	9378	9311	9232
Type 2	9381	9304	9240
Type 3	9316	9222	9111
Type 4	9359	9262	9162
Type 5	9166	9030	8887
Type 6	9205	9060	8915
Type 7	9026	8860	8702
Type 8	8439	8153	7891

Table 2
Ratio of perforated to solid infill plate strengths.

Perforation pattern	Nr	V_{op}/V_p from FE analysis		
		Perforation diameter		
		400 mm	500 mm	600 mm
Type 1	1	0.89	0.87	0.85
Type 2	2	0.89	0.87	0.85
Type 3	2	0.87	0.84	0.81
Type 4	2	0.88	0.85	0.83
Type 5	3.3	0.83	0.79	0.75
Type 6	3	0.84	0.80	0.76
Type 7	4	0.79	0.74	0.69
Type 8	7.3	0.62	0.54	0.46

to the columns (ω_{yci} and ω_{xci}) and beams (ω_{ybi} and ω_{xbi}) and (ω_{ybi-1} and ω_{xbi-1}) at any storey i can be determined from:

$$\omega_{xci} = (V_{op}/V_p)_i R_y F_y W (\sin \alpha_i)^2; \tag{9}$$

$$\omega_{yci} = (V_{op}/V_p)_i 0.5 R_y F_y W \sin 2\alpha_i$$

$$\omega_{xbi} = \omega_{xbi-1} + (V_{op}/V_p)_i 0.5 R_y F_y W \sin 2\alpha \tag{10}$$

$$\omega_{ybi} = \omega_{ybi-1} + (V_{op}/V_p)_i R_y F_y W (\cos \alpha)^2. \tag{11}$$

It is assumed that the distributed loads calculated in this way will act uniformly over the length of elements, although the magnitude changes between storeys.

- (3) The beam at any storey i is designed for distributed loads obtained from the difference between the tension forces developed in the infill plates at storey i and $i + 1$, namely, $\omega_{bi} = (V_{op}/V_p)_i (\omega_{ybi} - \omega_{ybi+1})$. The distributed loads are then combined with the gravity loads using appropriate load factors.
- (4) Axial forces in the beams can be estimated using the approach outlined in AISC Steel Design Guide 20. Axial forces are obtained from two sources: the first is due to the inward force from the infill plate applied to the columns, $P_{b(col)}$, and the second is from the difference in the effects of the infill plates above and below the beam, $P_{b(plate)}$. Thus, the axial force in the beam is

$$P_b = P_{b(col)} \pm P_{b(plate)}. \tag{12}$$

The axial force at the ends of the beam at storey i is

$$P_{bi} = \left(\omega_{xci} \frac{h_i}{2} + \omega_{xci+1} \frac{h_{i+1}}{2} \right) \pm (\omega_{xbi} - \omega_{xbi+1}) \frac{L}{2}. \tag{13}$$

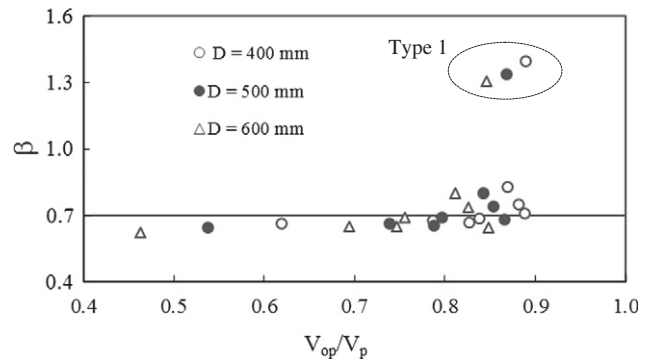


Fig. 10. Estimation of constant beta.

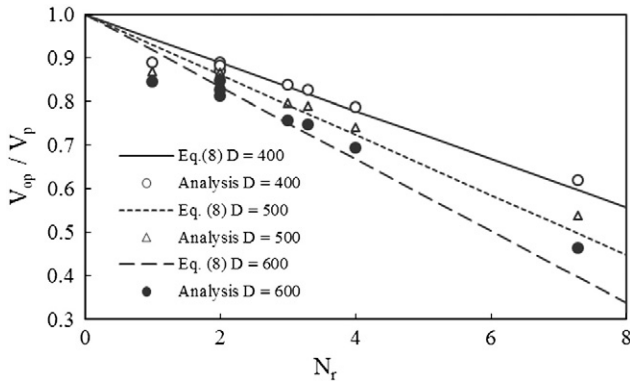


Fig. 11. Perforated to solid infill plate strength ratio (aspect ratio 2.0).

At the end where the column is in tension, the above two components of the axial force in the beams are additive.

- (5) All the beams are assumed to form a plastic hinge at their ends. The reduced plastic moment capacity at the ends of beam i , M_{pri} , can be obtained from the approximate equation [16]

$$M_{pri} = 1.18Z_{xi}F_{yb} \left(1 - \frac{P_{bi}}{A_{bi}F_{yb}} \right) \leq Z_{xi}F_{yb} \quad (14)$$

where Z_{xi} is the beam plastic section modulus, A_{bi} is the beam cross-sectional area, and F_{yb} is the beam yield strength.

Using the reduced plastic moment capacities, the shear forces at the ends of beam i , V_{bi} , can be obtained using the following equation:

$$V_{bi} = \frac{\sum M_{pri}}{L} \pm (\omega_{ybi} - \omega_{ybi+1}) \frac{L}{2} \quad (15)$$

where $\sum M_{pri}$ is the summation of the reduced plastic moment capacities at opposite ends of beam i .

With all the force components determined for the column free body diagrams, design axial forces for the columns can be easily calculated.

- (6) Column moments are calculated for each storey, assuming the beams are rigidly connected to the columns at each floor. The column moments, M_{col} , are calculated as the sum of those arising from infill plate tension and those from plastic hinging of the beams, as follows:

$$M_{col,i} = M_{plate,i} + \text{MAX}(M_{beam,i}; M_{beam,i-1}). \quad (16)$$

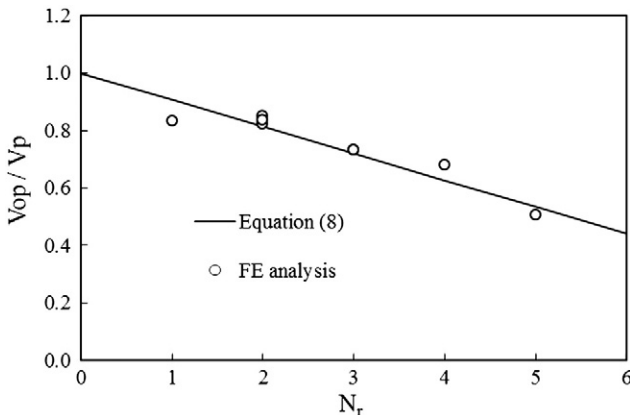


Fig. 12. Perforated to solid infill plate strength ratio (aspect ratio = 1.5).

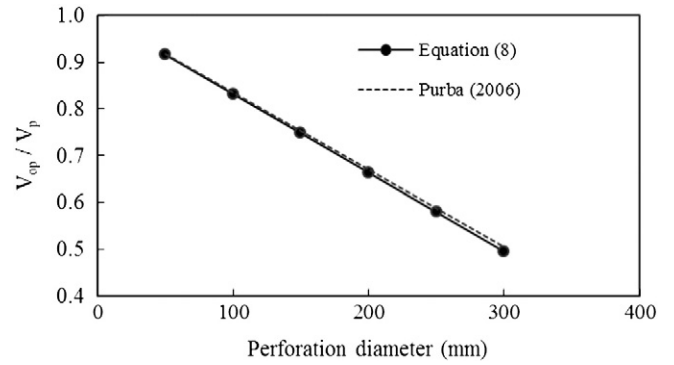


Fig. 13. Comparison of Eq. (8) with the equation proposed by Purba [6].

For a column assumed to be fixed against rotation at each end, the moment from the infill plate tension field is

$$M_{plate,i} = \frac{\omega_{xci} h_i^2}{12} \quad (17)$$

where ω_{xci} is calculated from Eq. (8). For the moment due to plastic hinging in the beam, $M_{beam,i}$ or $M_{beam,i-1}$, one-half of the reduced plastic moment of the beam can be applied to each column segment connected to that beam (i.e., above and below). Similar to AISC Steel Design Guide 20 [7], the column moments at the top and bottom storeys are taken as the moment due to plastic hinging at the ends of the beam.

5. Design example

Three 4-storey SPSWs were selected to evaluate the accuracy of the proposed design method. The 4-storey building is assumed to have the same plan area as the building considered earlier. The building has two identical 4-storey SPSWs to resist lateral forces in one direction. Each

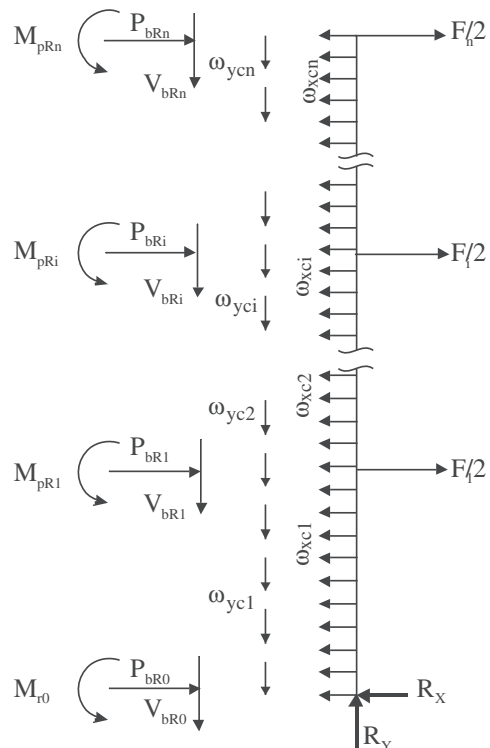


Fig. 14. Free body diagram of typical right column of a SPSW.

shear wall is 5.7 m wide with an aspect ratio of 1.5 (storey height of 3.8 m). A dead load of 4.26 kPa was used for each floor and 1.12 kPa for the roof. The live load on all floors was taken as 2.4 kPa. Design seismic loads at every storey were calculated using the equivalent static force procedure of NBCC 2010 [12]. The base shear for one 4-storey SPSW was calculated as 1150 kN. Distribution of the base shear over the height of the SPSW resulted in lateral loads of 155 kN, 311 kN, 466 kN, and 217 kN, at each storey from the first to the fourth, respectively. Two types (Type 5 and Type 6) of perforations are selected in this study. For Type 5 perforation only variable plate thickness (4-storey SPSWT5VT) over the height of the SPSW is considered and for Type 6 perforations variable infill plate thicknesses (4-storey SPSWT6VT) as well as constant infill plate thickness are considered (4-storey SPSWT6CT). The selected perforated 4-storey SPSWs are shown in Figs. 15 and 16. A yield strength of 385 MPa was selected for the infill plates, whereas the yield strength for the beams and columns was taken as 350 MPa. All steel members were assumed to have a modulus of elasticity of 200 000 MPa.

For the perforation patterns selected for these sample calculations, a value of 3 was used for N_r value. From Eq. (8), the value of $V_{op}/V_p = 0.72$ was calculated. The preliminary selection of beams and columns was based on the design loads that were obtained after the first iteration of the proposed method with an assumed tension field inclination angle of 45° . The calculations for the second iteration are described in the following only for the variable plate thickness case. The distributed forces, obtained from yielding of the infill plates, were obtained from Eqs. (9), (10) and (11) and are presented in Table 3. The angle of inclination of the tension field presented in Table 3 was obtained from the equation in CAN/CSA-S16-09.

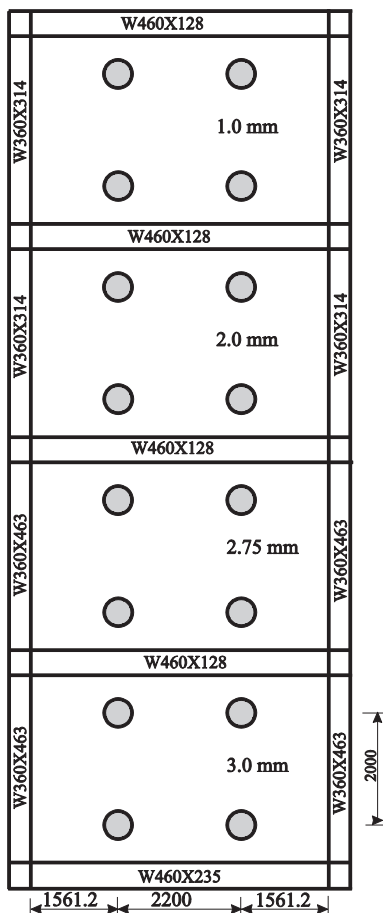


Fig. 15. 4-storey SPSW with Type 5 perforations.

Axial forces for the beams of the 4-storey SPSWVT were calculated using Eq. (13) and are summarised in Table 4. The values of P_{bL} and P_{bR} are the axial force at the beams left and right ends, respectively. The reduced plastic moments for the selected beam sections were calculated using Eq. (14). Using the reduced plastic moment capacity of the beams (M_{pRL} and M_{pRR}), shear forces at the left and at the right ends of the beams (V_{bL} and V_{bR}) were calculated using Eq. (15). Table 4 also tabulates the reduced plastic moments and shear forces at the left and right ends of all beams for the 4-storey perforated SPSW with variable plate thicknesses.

Finally, axial forces and bending moments in the boundary columns in every storey were calculated for both SPSWs with variable plate thicknesses and constant plate thicknesses and are presented in Table 5.

6. Evaluation of shear strength equation for perforated shear wall

Nonlinear pushover analysis was conducted for the two 4-storey perforated SPSWs with variable infill plate thickness (4-storey SPSWT5VT and 4-storey SPSWT6VT) and the proposed shear strength equation was evaluated by comparing the shear strengths of the perforated infill plates to solid infill plates. Pushover analyses were also conducted for 4-storey solid SPSW with variable infill plate thickness. A target displacement of 500 mm at the top of the SPSW was used for all pushover analysis. Ratios of perforated infill plate strengths to the solid infill plate strength, V_{op}/V_p , were calculated for both 4-storey perforated SPSWs and are presented in Table 6. From Eq. (8), the value of $V_{op}/V_p = 0.72$ was calculated as 0.72 for both the selected SPSWs (4-storey SPSWT5VT and SPSWT6VT). The average V_{op}/V_p ratio obtained from the FE analysis is 0.74 for 4-storey SPSWT5VT, which is about 2.7% higher than the value predicted from Eq. (8). For 4-storey SPSWT6VT, the average V_{op}/V_p ratio obtained from the FE analysis is 0.75, which is about 4% higher than the value predicted from Eq. (8). The maximum difference between the FE analysis result and the predictions from Eq. (8) was observed at the fourth storey for the 4-storey perforated shear wall with Type 6 perforation pattern (4-storey SPSWT6VT) and was approximately 6.9%. Thus, the proposed shear strength equation, Eq. (8), can be used for calculations of shear strengths of infill plates of multistorey SPSWs with circular perforations.

7. Comparison with seismic analyses

Four different seismic records were chosen for the time history response analysis. These are: (1) N-S component of the El Centro earthquake of 1940; (2) Petrolia station record from the 1992 Cape Mendocino earthquake; (3) Nahanni, Canada 1985 earthquake record; and (4) Parkfield 1966 earthquake record. The seismic records were modified using the software SYNTH [17] to make them spectrum compatible for Vancouver, Canada. Nonlinear time step dynamic analyses of the 4-storey SPSWs were performed using ABAQUS [11]. The finite element model includes one steel plate shear wall and a gravity “dummy” column carrying the vertical load supported by half of the leaning columns in the building. The gravity column consists of a rigid bar pinned at its base and connected to the steel plate shear wall at every storey with pin-ended rigid links. The boundary conditions and material properties are the same as for the single storey SPSWs described earlier. In the finite element analyses, the storey gravity loads were represented as lumped masses on the columns at every floor. Rayleigh proportional damping with a ratio of 5% was selected for all the seismic analyses.

Axial forces and bending moments for the boundary columns of the 4-storey perforated SPSWs were obtained from nonlinear seismic analysis. Figs. 17 to 19 present the envelopes of absolute maximum column axial forces and column moments obtained from the seismic analyses. It is observed that for all the three selected walls, for all ground motions, the axial forces in every storey are lower than the design axial forces obtained from the proposed method. The proposed design forces for

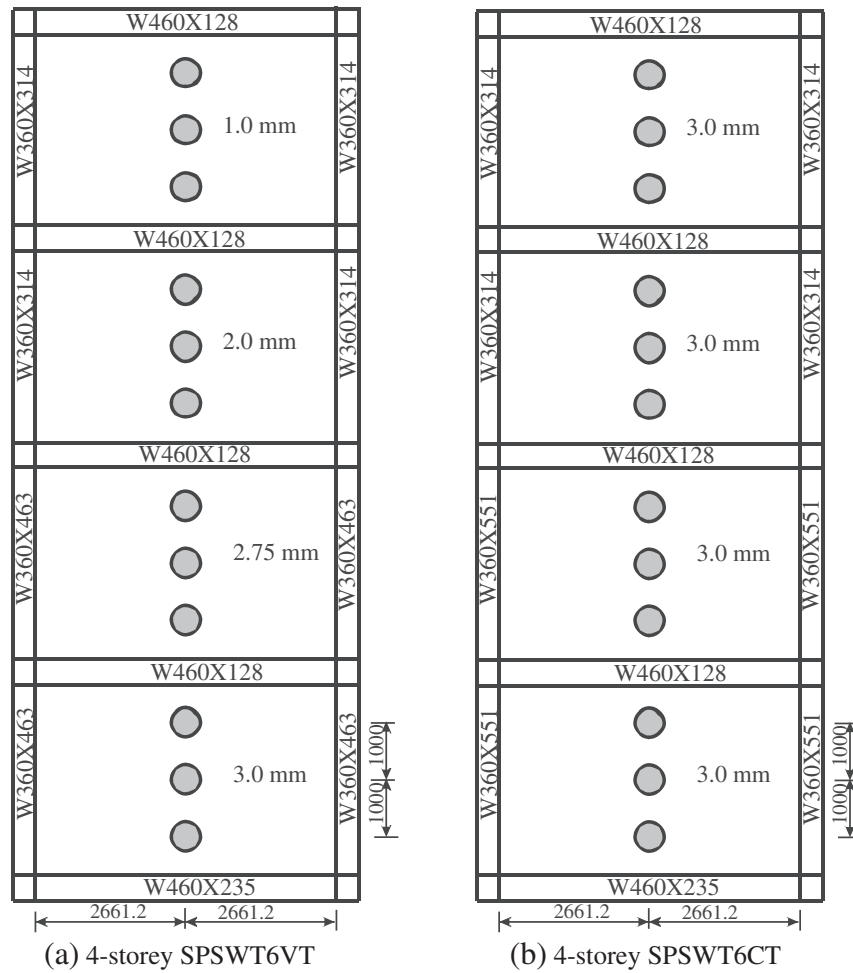


Fig. 16. 4-storey SPSWs with Type 6 perforations.

shear walls with variable infill plate thickness (4-storey SPSWT5VT and 4-storey SPSWT6VT) are identical since in each case three strips are discounted. For the 4-storey SPSWT5VT specimen, the maximum column axial force obtained from the time history analyses is 7450 kN for the Petrolia 1992 earthquake record, which is only 3.3% lower than the proposed design axial force of 7700 kN. For the 4-storey SPSWT6VT shear wall (Fig. 18) the maximum column axial force obtained from the time history analyses is 7460 kN for the Petrolia 1992 earthquake record, which is only 3.1% lower than the proposed design axial force. Figs. 17 and 18 show that the peak seismic demand for flexure at the base of the columns of the 4-storey SPSWT5VT specimen is 1340 kN·m for the Petrolia 1992 earthquake record, and 1322 kN·m for the 4-storey SPSWT6VT under the Nahanni 1985 earthquake record. These moments are lower than the proposed design moment of 2040 kN·m. The design column moments for the upper storeys are

Table 3
Distributed loads from perforated infill plates for 4-storey SPSWVT.

Storey	α (degrees)	Loads from yielding infill plates (kN/m)		
		ω_{yc} and ω_{yb}	ω_{xc}	ω_{yb}
1	42.9	415	385	447
2	41.0	378	329	434
3	41.9	276	247	308
4	43.2	138	130	147

also much larger than the column moments determined from the seismic analyses.

Fig. 19 shows that, for the 4-storey shear wall with constant infill plate thickness, SPSWT6CT, the maximum column axial force developed

Table 4
Beam end forces of 4-storey SPSWVT.

Beam	P_{bL} (kN)	P_{bR} (kN)	M_{pRL} (kN·m)	M_{pRR} (kN·m)	V_{bL} (kN)	V_{bR} (kN)
Base	1180	-1180	2040	2040	1900	-465
1	-1460	-1250	939	985	300	375
2	-1380	-803	956	1070	-5	715
3	-1110	-325	1020	1070	-91	822
4	-641	148	1070	1070	-46	795

Table 5
Design column forces for 4-storey SPSWs.

Storey	4-storey SPSWT T5VT/T6VT		4-storey SPSW T6CT	
	Column axial force (kN)	Column moment (kN·m)	Column axial force (kN)	Column moment (kN·m)
1	7703	2044	9310	2044
2	5630	929	7353	909
3	3356	831	5294	923
4	1356	1224	3208	1536

Table 6
Ratios of perforated to solid infill plate strengths for multistorey SPSWs.

Storey	Solid plate shear V_p (kN)	4-storey SPSWT5VT		4-storey SPSWT6VT	
		Perforated plate shear V_{op} (kN)	$\frac{V_{op}}{V_p}$	Perforated plate shear V_{op} (kN)	$\frac{V_{op}}{V_p}$
1	3043	2224	0.73	2201	0.72
2	2821	2085	0.74	2102	0.75
3	2052	1538	0.75	1521	0.74
4	992	722	0.73	759	0.77
Mean			0.74		0.75

at the base from the time history analyses, 7450 kN for the Petrolia 1992 earthquake record, is 20% lower than the proposed design axial force, 9310 kN. Also, the peak seismic demand for flexure at the base of the columns, 1343 kN·m for the Petrolia 1992 earthquake record is 34% lower than the proposed design moment of 2040 kN·m.

One of the objectives of introducing perforations in infill plates was to reduce their strength and, thereby, reduce the seismic demand on the boundary columns of SPSWs. To demonstrate how perforations help reduce the seismic demand on columns, seismic analysis for the 4-storey solid SPSW (with no perforations) with variable infill plate thickness was conducted using the El-Centro earthquake record. The results from the seismic analysis are compared with the results from two perforated SPSWs (4-storey SPSWT5VT and 4-storey SPSWT6VT) in Fig. 20. Fig. 20 shows that the axial forces in every storey of the solid SPSW are higher than those for the two selected SPSWs with perforations. The column axial force at the base of the solid SPSW, 8175 kN, is 15.8% higher than that for 4-storey SPSWT5VT (6886 kN) and 16.5% higher than that for 4-storey SPSWT6VT (6829 kN). Fig. 20 also shows that the maximum bending moment at the base of the column of the solid SPSW, 1368 kN·m, is 7.8% higher than the column moment for 4-storey SPSWT5VT (1261 kN·m) and 10.4% higher than that for 4-storey SPSWT6VT (1226 kN·m). Thus, perforation in SPSW significantly decreases the seismic demand at boundary columns of SPSW.

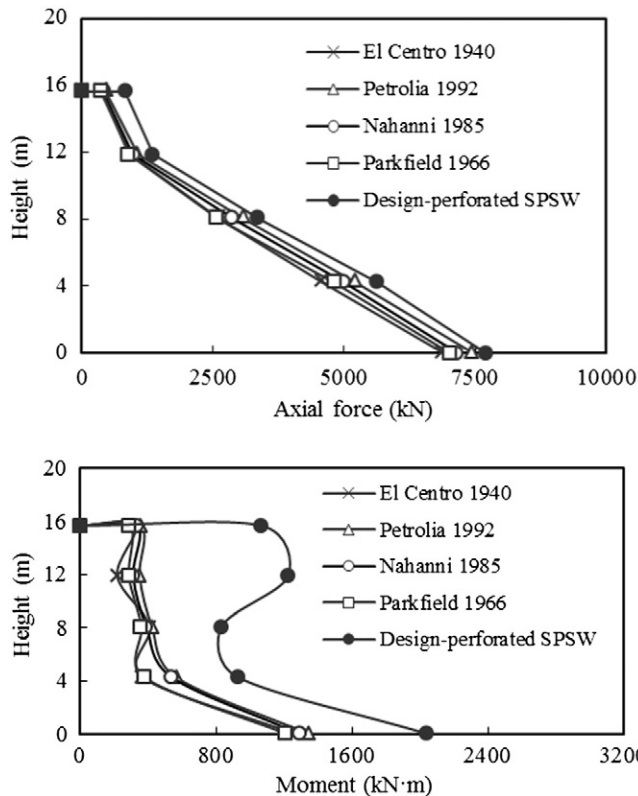


Fig. 17. Peak column axial forces and moments for 4-storey SPSWT5VT.

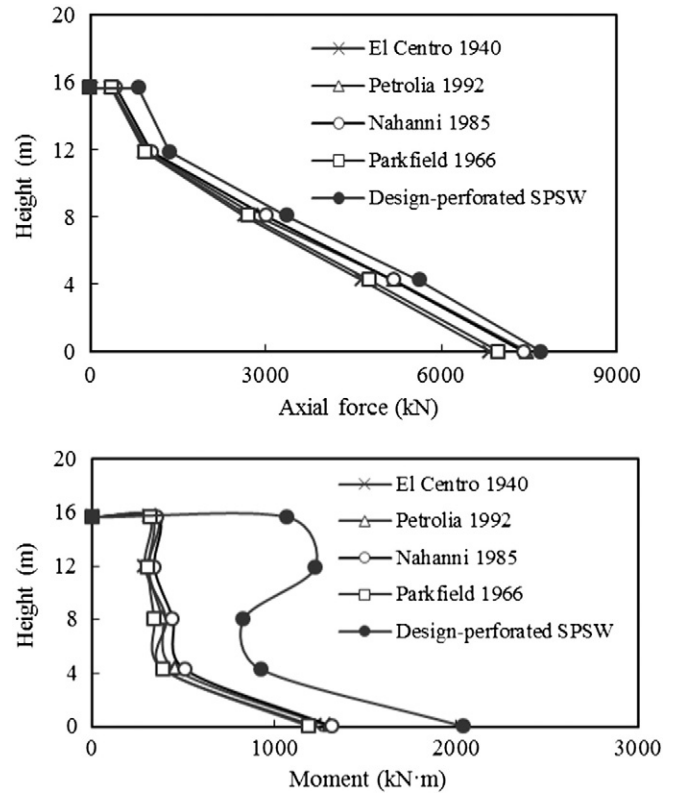


Fig. 18. Peak column axial forces and moments for 4-storey SPSWT6VT.

Summary and conclusions

A series of finite element analyses of unstiffened SPSWs with different perforation patterns were performed. The analyses show that the

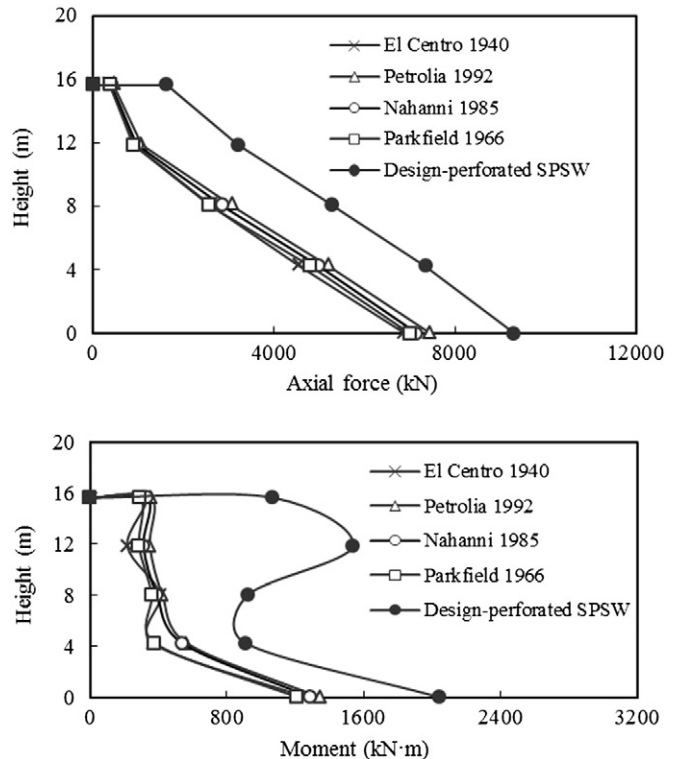


Fig. 19. Peak column axial forces and moments for 4-storey SPSWT6CT.

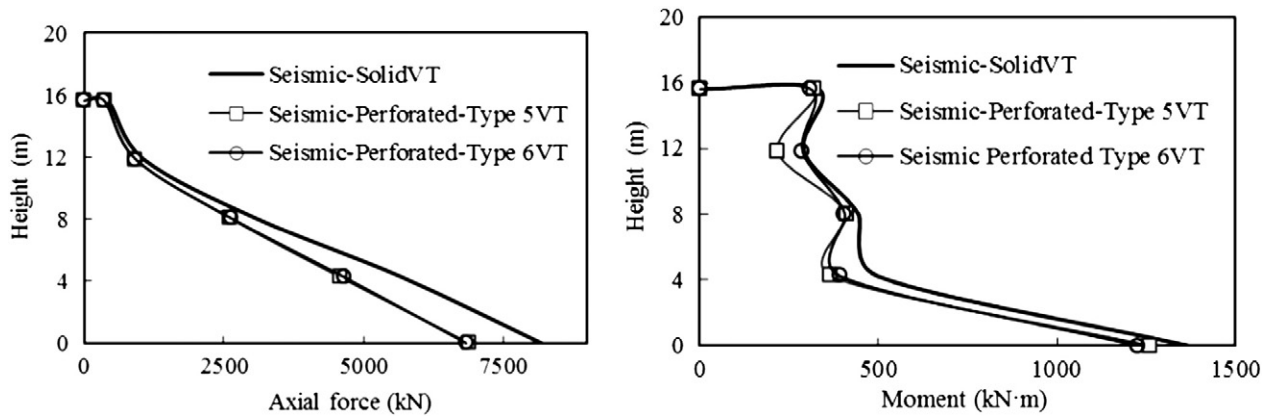


Fig. 20. Column forces for 4-storey SPSW with variable plate thickness under El-Centro earthquake.

shear strength of an infill plate with circular perforations can be calculated by reducing the shear strength of the solid infill plate by the factor given by Eq. (8). The equation was found to give excellent predictions of reduced shear strengths of SPSWs with different patterns of perforations, different perforation diameters, and different infill plate aspect ratios.

A procedure for calculating the design force effects for columns of perforated SPSWs is proposed. Design column axial forces from the proposed procedure were shown to agree very well with the results of nonlinear seismic analyses of three 4-storey SPSWs with circular perforations in the infill plates. The predicted design column moments were larger than the moments obtained from seismic analysis. This was mainly because the design earthquake records used for the analysis did not cause plastic hinging at the end of the beams as assumed in the capacity design approach.

It is recognised that the proposed shear strength equation for perforated SPSW is derived based on analysis of limited number (a total of 32) of perforated shear walls. It is suggested that the proposed formula be re-evaluated with more analysis results on SPSWs with wider variety of geometries and different perforation patterns. Also, use of seismic records with longer durations and of larger magnitudes is recommended for seismic evaluation of the proposed design method.

Acknowledgements

This work was supported by the Steel Structures Education Foundation and the Faculty of Engineering and Computer Science, Concordia University, Montreal, Canada. Their support is gratefully acknowledged.

References

- [1] Berman JW, Bruneau M. Experimental investigation of light-gauge steel plate shear walls. *ASCE J Struct Eng* 2005;131(2):259–67.
- [2] Vian D. Steel plate shear walls for seismic design and retrofit of building structures. PhD dissertation Buffalo, Buffalo, N.Y.: State Univ. of New York; 2005.
- [3] Hitaka T, Matsui C. Experimental study on steel shear walls with slits. *ASCE J Struct Eng* 2003;129(5):586–95.
- [4] Cortes G, Liu J. Experimental evaluation of steel slit panel–frames for seismic resistance. *J Constr Steel Res* 2011;67(2):181–91.
- [5] Roberts TM, Sabouri-Ghomi S. Hysteretic characteristics of unstiffened perforated steel plate shear panels. *Thin Walled Struct* 1992;14:139–51.
- [6] Purba RH. Design recommendations for perforated steel plate shear walls. [M.Sc. Thesis] Buffalo, N.Y.: State University of New York at Buffalo; 2006.
- [7] Sabelli R, Bruneau M. Steel design guide 20: steel plate shear walls. Chicago, IL: American Institute of Steel Construction; 2007.
- [8] Canadian Standards Association. CAN/CSA-S16-09. Toronto, Ontario, Canada: Limit States Design of Steel Structures; 2009.
- [9] AISC. Seismic provisions for structural steel buildings. Chicago, IL: American Institute of Steel Construction; 2010.
- [10] Thorburn LJ, Kulak GL, Montgomery CJ. Analysis of steel plate shear walls. Structural Engineering Report No. 107. Edmonton, AB: Dept. of Civil Engineering, University of Alberta; 1983.
- [11] Hibbit, Karlsson and Sorensen. ABAQUS/standard user's manual. Version 6.7. Pawtucket, RI: HKS Inc.; 2007.
- [12] NBCC. National building code of Canada. Ottawa, ON, Canada: National Research Council of Canada (NRCC); 2010.
- [13] Shishkin JJ, Driver RG, Grondin GY. Steel plate shear walls using the modified strip model. Structural Engineering Report No. 261. Edmonton, Canada: Department of Civil and Environmental Engineering, University of Alberta; 2005.
- [14] Bhowmick AK, Grondin GY, Driver RG. Performance of type D and type LD steel plate shear walls. *Can J Civ Eng* 2010;37(1):88–98.
- [15] Bhowmick AK, Grondin GY, Driver RG. Estimating fundamental periods of steel plate shear walls. *Eng Struct* 2011;33:1883–93.
- [16] Bruneau M, Whittaker AS, Uang CM. Ductile design of steel structures. New York: McGraw-Hill; 1998.
- [17] Naumoski N. Program SYNTH-generation of artificial accelerogram history compatible with a target spectrum. User's manual. Ottawa, ON, Canada: Dept. of Civil Engineering, University of Ottawa; 2001.